International Conference 'Wind Effects on Trees'
September 16-18, 2003, University of Karlsruhe, Germany

Calibration and Applications of a Shelterbelt Turbulent Flow Model

E.S. Takle[(1)], M.J. Falk[(1)], X. Zhou[(2)], and J.R. Brandle[(2)]
[(1)] Iowa State University, Ames, IA 50010 USA
[(2)] University of Nebraska-Lincoln, Lincoln, NE 68588 USA

Abstract

An atmospheric boundary layer turbulence model for flow through shelterbelts was calibrated by use of field data. A mature tree shelterbelt was disassembled to provide a two-dimensional representation of surface area per unit volume, a key parameter used by the model to characterize the drag force produced by the vegetation. The calibrated model provided agreement with observed pressure and velocity both upwind and downwind of the shelter to approximately 22%. Other applications of the model include simulating high wind speed flows, pollen dispersion, and particle transport.

Introduction

We have developed a model for turbulent flow through vegetation that uses plant surface area per unit volume as a means of describing the drag force that extracts momentum from the flow. Because the momentum extracted is proportional to the square of the wind speed, accuracy is needed in numerical simulation of the wind speed locally within the porous barrier. This requires solution of the full Navier-Stokes equations at numerous points within the vegetation. However, the presence of solid material in the solution domain calls for special care in use of the Navier-Stokes equations for this application. These issues are addressed by Wang et al (2001).

In this paper we describe results of calibrating the model against actual measurements of surface area per unit volume for a vegetative barrier consisting of a line of trees used as a shelterbelt in an agricultural area. Once the model has been fully tested against actual measured flow fields it can be applied to numerous problems such as assessing forces on vegetation in high wind speed environments and transport of pollen, odor, particulates, or snow. Earlier studies of wind modification by natural barriers are well summarized by Van Eimern et al (1964), Rosenberg (1979), McNaughton (1988), and Heisler and Dewalle (1988). More recent studies also explore the effects of artificial barriers on wind and climate, as seen in Bradley and Mulhearn (1983), McAneney and Judd (1987, 1991) and Wilson (1985, 1987, 1997).

Measurements

Measurements of meteorological conditions and leaf area per unit volume were made during the summers of 2000 and 2001 at the University of Nebraska Agricultural Research and Development Center north of Lincoln, Nebraska USA. Meteorological measurements were

made near a two-row shelterbelt of Green Ash, Austrian Pine, and Eastern Red Cedar trees of height (H) 12 m at its tallest point and width 12 m at its widest point that was oriented east-west with unobstructed fetch to the south (direction of the prevailing wind). Wind speeds used in the current study were taken from Young 12005 3-cup anemometers located at heights of 0.25 H (3 m), 0.5 H (6 m), and 1.0 H (12 m) on towers 1.5 H (18 m) upwind of the shelterbelt and 1.5 H (18 m), 3.0 H (36 m), 4.5 H (54 m), and 6.0 H (72 m) downwind of the shelterbelt. Measurements represent 10-minute averages taken simultaneously. Leeward velocities were normalized by the (undisturbed) windward velocities at the same height. Wind speeds used for this calibration ranged from 6 to 8 m s^{-1}. Measurements used in this calibration were for winds perpendicular to the barrier to allow for use of a two-dimensional model domain.

Pressure difference was measured at ground level by the Setra Systems 264 Series transducer pressure sensors each having one side connected by automobile vacuum tubing to a port open at the base of one of the towers (and other locations between) and the other side connected to a reference port about 100 m upwind of the barrier. Details are contained in Takle et al (1997). The shelterbelt descriptor was leaf area density (A), which is defined as the surface area of plant material per unit volume. Values within the shelter ranged from nearly zero to over 3 m^2m^{-3}. Eighteen trees similar to those in the shelterbelt were disassembled in 1996 and 1997, and their lengths, middle diameters, surface areas, and volumes were determined. This plant material provided an accurate picture of the actual composition of trees in the shelterbelt. These data were converted into a set of equations and a standard profile by Zhou et al (2002), which is the leaf area density profile used by our model, as shown in Fig. 1.

Height (m)										
		0	0	0.15	0.12	0	0	0	0	
	12	0	0.42	0.63	0.45	0.19	0.23	0	0	
		0	1.11	1.66	1.2	0.44	0.61	0.41	0	
	10	0	1.93	2.91	2.09	1.06	1.48	0.98	0	
		1.49	2.45	2.76	1.97	1.91	2.66	1.77	0	
	8	1.64	2.7	3.06	2.17	1.84	2.58	2.29	1.39	
		1.69	2.78	3.17	2.23	2.06	2.91	2.56	1.56	
	6	1.61	2.65	3.05	2.13	2.07	2.95	2.58	1.57	
		1.46	2.39	2.79	1.92	1.95	2.82	2.43	1.48	
	4	1.24	2.03	2.42	1.63	1.71	2.5	2.12	1.29	
		0	1.57	2.53	1.7	1.36	2.05	1.69	1.03	
	2	0	1.08	1.84	1.17	1.26	1.95	1.17	0	
		0	0.59	1.14	0.64	0.7	1.21	0.65	0	
	0	0	0	0.86	0	0	0.92	0	0	
		0	1.5	3	4.5	6	7.5	9	10.5	12
		Width (m)								

Figure 1. Leaf-area density (m^2 m^{-3}) in 1m x 1.5 m (vertical x horizontal) grid cells for a cross-section of an agricultural shelterbelt.

The small values in the top row of the chart show that a very small amount of leaf area is at a height of greater than 12 m, but we still consider the height of the shelter to be 12 m.

Leaf area density is related to resistance coefficient by:

$$k_r = \int_{-\infty}^{\infty} C_d A dx \quad (1)$$

where k_r is the resistance coefficient, C_d is the drag coefficient, A is the leaf area density, and x is the distance through the shelterbelt.

Model

The Reynolds-Averaged Navier-Stokes model used to simulate this turbulent flow in and around the vegetation is described by Wang and Takle (1995). The model is quasi-three-dimensional, meaning that it is assumed that the barrier is infinitely long in the y-direction and that all variables in that direction remain constant throughout the domain.

$$\frac{\partial u}{\partial t} = -\frac{1}{\rho}\frac{\partial p}{\partial x} - u\frac{\partial u}{\partial x} - w\frac{\partial u}{\partial z} - \frac{\partial \overline{u'^2}}{\partial x} - \frac{\partial \overline{u'w'}}{\partial z} - C_d A U u \quad (2)$$

$$\frac{\partial w}{\partial t} = -\frac{1}{\rho}\frac{\partial p}{\partial z} - u\frac{\partial w}{\partial x} - w\frac{\partial w}{\partial z} - \frac{\partial \overline{u'w'}}{\partial x} - \frac{\partial \overline{w'^2}}{\partial z} - C_d A U w \quad (3)$$

$$\frac{\partial u}{\partial x} + \frac{\partial w}{\partial z} = 0 \quad (4)$$

where u and w are the mean wind speed components in the x- and z- directions, and where u' and w' are perturbations about the mean wind speed. Pressure is abbreviated by p, density by ρ, and the total mean wind speed by U. The drag coefficient, which is abbreviated C_d, is determined empirically by comparison of modeled with measured wind speeds.

The turbulence terms in the two-dimensional equations of motion are solved by a second-order closure scheme proposed by Mellor and Yamada (1974). Inflow boundary conditions were supplied by the windward towers (extrapolated vertically by a logarithmic profile to the model top). Outflow boundary conditions are set so that the normal derivatives of velocity and pressure are zero. Vertical derivatives of u, w, p, and turbulence kinetic energy are specified at the top boundary. The bottom boundary is also subject to defined vertical pressure gradients and a no-slip condition (u = w = 0) (Wang and Takle 1995). Equations for motion, mass conservation, turbulence kinetic energy, and mixing length are discretized into a set of tridiagonal matrices and solved simultaneously by an Alternating Direction Implicit scheme (Wang and Takle 1995). The dynamic pressure perturbations are solved by use of auxiliary velocity fields as shown in Chorin (1968) and solved by the successive overrelaxation method to accelerate convergence.

The domain for the shelter herein reported (H = 12 m) extended 200 m upwind of the shelter, 400 m downwind of the shelter, and had height 100 m. Horizontal resolution was 1.5 m and vertical resolution was 1 m. Effects of low vegetation upwind and downwind of the major barrier were incorporated by use of an assumed surface roughness length. Simulations with numerous domain sizes confirmed that the domain reported herein had minimal influence on simulated conditions near the barrier.

Results

A time period was selected that had consistent, strong winds (approximately 8 m s^{-1}, which was the simulated incident wind speed at the top of the shelter) nearly perpendicular to the shelterbelt. Over an hour of observations were taken and averaged. Each observation was normalized by the undisturbed upwind velocity at its height. The events were simulated with the model, and the results were normalized in the same way. Five towers each taking observations at three heights gives fifteen normalized observations with which to compare the model.

The optimal drag coefficient was determined empirically by comparing wind speeds at the 15 tower locations with modeled values at these locations and minimizing the mean absolute error. The value of C_d that gave minimum absolute error was 0.23, so this value was used for all subsequent simulations of barriers of this type.

When the model was run with 0.23 as the drag coefficient, the mean absolute error was 0.10, meaning that both the model and observations were normalized by their undisturbed upwind velocities and that the two normalized velocities differed on average by 0.10. If we normalize each difference by the observed value, we obtain an average error of 22% between the model and observations.

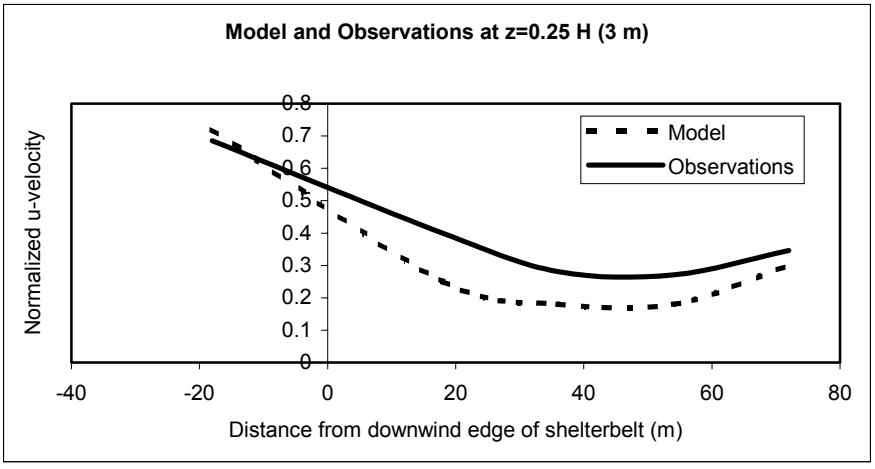

(a)

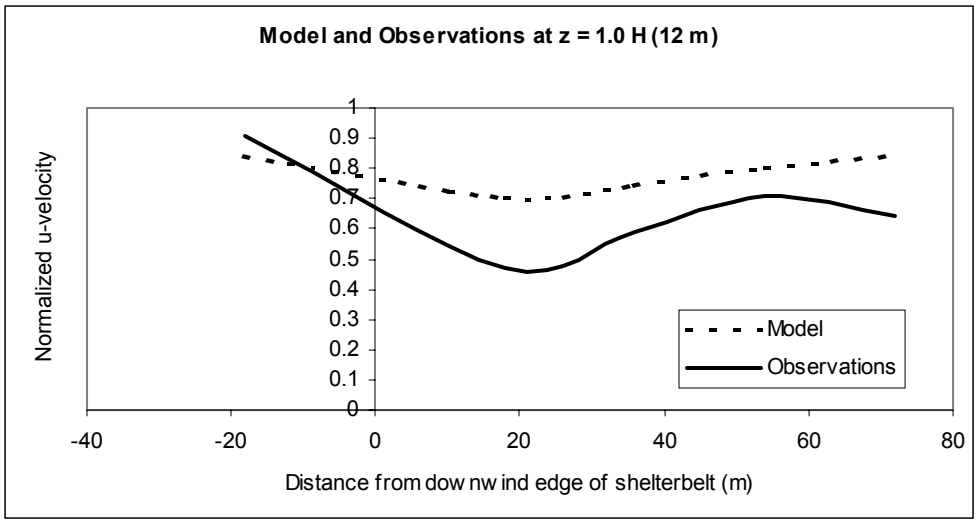

(b)

Figure 2. Normalized horizontal wind speed at (a) 3 m and (b) 12 m from observations and model simulations of flow though a vegetative barrier.

Since the velocities were each normalized by undisturbed upwind speeds at their own levels, the wind speeds at lower heights and in the near lee were normalized by a lower number. This has the effect of magnifying errors where the shelter has the most influence.

To validate the model with the new drag coefficient, we compared predicted and observed pressure fields. Key features of the field both upwind and downwind of the shelterbelt were captured by the model. The pressure peak occurs at nearly exactly the same location with relation to the shelterbelt, as does the pressure drop behind the trees. The magnitude of the peak and fall are nearly the same, though the model has higher pressure in front of the shelter than was observed. Applications of the model to events on days other than the calibration day produced results similar to those of Figure 2.

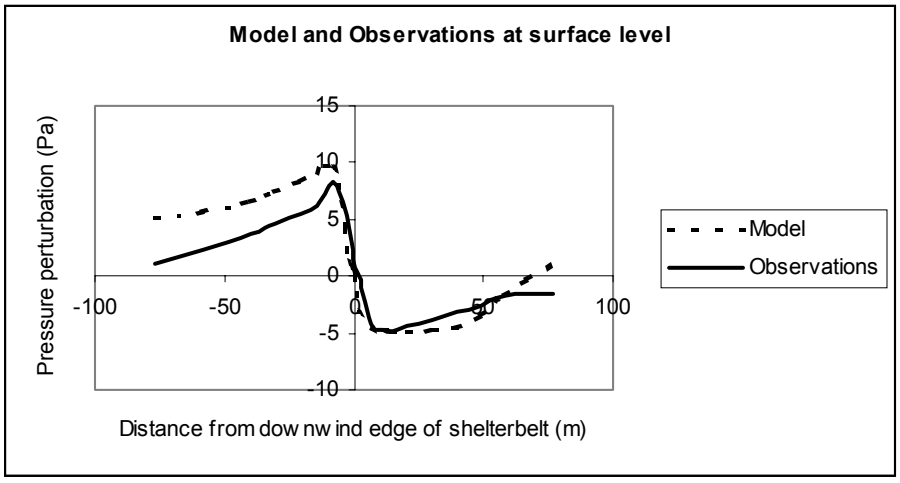

Figure 3. Horizontal distribution of surface pressure difference from the reference location.

Discussion

Sources of error may include the difference between the disassembled shelterbelt and the shelterbelt used for field observations. Both were two-row shelters consisting of Green Ash, Eastern Red Cedar, and Austrian Pine trees with similar lengths, widths, and heights. Additionally, since each individual tree has a unique distribution of surface area, an average profile must be used to simulate trees, so deviations from the normal in each individual tree are not considered by the model.

Additionally, different parts of trees have different aerodynamic properties, including drag coefficient. The tops of the trees consist almost solely of leaves, whereas at lower levels a greater portion of the mass consists of woody material, and thus drag is exerted differently at high and low levels. Orientation to the wind and distribution of plant material for individual trees therefore can affect the wind profile. A possibility future model refinement would allow separate drag coefficients for leaves, branches, and trunks, provided data on distributions of these characteristics is known for the barrier.

As wind speeds increase, the trees also sway in the wind, whereas the model does not allow momentum transfer to tree motion. The motion of the trees changes the drag characteristics of a shelterbelt. The kinetic energy of the trees, however, is several orders of magnitude smaller than that of the wind simply because the trees do not move quickly, even though their mass is large. With speeds larger than those we simulated, however, phenomena such as wind throw would need to be investigated.

Since the cup anemometers were aligned to measure wind parallel to the ground, sensors located at points with large vertical winds may not have accurately resolved the horizontal component. No correction was made for wind components reported when the mean wind is not in the plane of rotation of the cups.

The model also is affected by truncation error. Many of the differencing schemes used by the model are second-order accurate, which introduces small errors. Rounding errors by the processor which runs the model also must be considered. Individual calculations have only small errors, but the model for some configurations requires hundreds of thousands of iterations to achieve a steady state solution, thereby providing opportunity for error growth.

The shelterbelt model assumes that the landscape away from the barrier is reasonably flat and smooth. Aerodynamically rough surfaces or crops in the vicinity of the barrier can be accommodated in two ways. First, the surface roughness length may be increased. The roughness length accounts for the crops by raising the level at which velocity goes to zero. Secondly, tall crops may be assigned a leaf area density and in effect become a part of the vegetative barrier in the model. These modifications can improve the results when the shelterbelt model is used to simulate landscapes that are not flat and bare.

The model has also been tested using high wind speeds ordinarily accompanying most extreme weather events. Pressure, drag, and turbulence kinetic energy all increase dramatically with an

increase in velocity, which can create effects on the barrier itself. For an incident velocity of 30 m s^{-1}, as shown in Fig. 4, the pressure difference can exceed 200 Pa across the barrier, both aloft and at the surface. At the surface and at 0.8 H (approximately 10 m), the pressure fields are nearly identical and create very severe pressure gradient forces.

Such strong pressure gradients serve to accelerate the flow even more as it passes through and over the shelterbelt, creating strong overspeeding over the top of the shelterbelt while also creating an intense velocity decrease below the top of the shelterbelt.

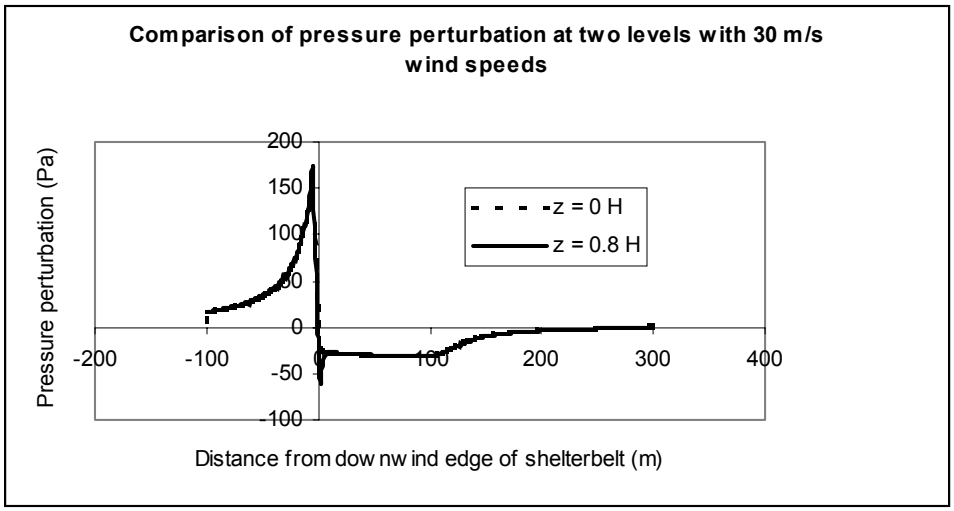

Figure 4. Pressure perturbation simulated as a function of distance downwind of he leeward edge of the shelter.

The pressure at the ground and at 0.8 H is nearly identical, even for a high wind speed such as 30 m s^{-1}. The surface pressure, therefore, provides a reasonable approximation of the pressure at the top of the shelter.

Future Applications

The model also has been used to produce flow fields to drive a Lagrangian particle transport model used to simulate pollen dispersion for assessing environmental impact of genetically modified crops (Arritt et al 2002). Additional possible applications include simulations of transport and diffusion of odors, suppression of pesticide drift from agricultural sprayers, soil erosion by wind, snow accumulation, and particle transport and dispersion.

Acknowledgments

One of us (M.J. Falk) acknowledges financial support of the Iowa State University Agronomy Department Endowment Fund. Support also was provided by the USDA NRI Competitive Grants Program (Contract 96351083892).

References

Arritt, R.W., Westgate, M.E., Riese, J.M., Takle, E.S., and Falk, M.J., 2002: "A Coupled Physical-Biological Model for Maize Pollination", 15th Conf. on Biometeorology/Aerobiology and 16th Congress of Biometeorology, American Meteorological Society, Kansas City, Mo, 28 October-1 November 2002.

Arritt, R.W., Riese, J.M., Westgate, M.E., Takle, E.S., and Falk, M.J., 2002: "Application of a Lagrangian model for pollen dispersion. 15th Conference on Boundary Layer and Turbulence. American Meteorological Society, Wagenigen, Netherlands, 15-19 July 2002.

Bradley, E.F. and P.J. Mulhearn, 1983: "Development of Velocity and Shear Stress Distributions in the Wake of a Porous Shelter Fence", Journal of Wind Engineering and Industrial Aerodynamics 15, 145-156.

Chorin, A.J., 1968: "Numerical solution of the Navier-Stokes equations", Mathematics of Computation 22, 745-762.

Heisler, G.M. and Dewalle, D.R., 1988: "Effects of Windbreak Structure on Wind Flow", Agriculture, Ecosystems and Environment 22/23, 41-69.

McAneney, K.J. and Judd, M.J., 1987: "Comparative Shelter Strategies for Kiwifruit: a Mechanistic Interpretation of Wind Damage Measurements", Agricultural and Forest Meteorology 39, 225-240.

McAneney, K.J. and Judd, M.J., 1991: "Multiple Windbreaks: an Aeolian Ensemble", Boundary Layer Meteorology 54, 129-146.

McNaughton, K.G., 1988: "Effects of Windbreaks on Turbulent Transport and Microclimate", Agriculture, Ecosystems, and Environment 22/23, 17-39.

Mellor, G.L. and Yamada, T., 1974: "A Hierarchy of Turbulence Closure Models for Planetary Boundary Layers", Journal of Atmospheric Science 31, 1791-1806.

Rosenberg , N.J., 1979: "Windbreaks for Reducing Moisture Stress", Modification of Aerial Environment of Plants, edited B.J. Barfield and J. F. Gerber. 538 pp.

Takle, E.S., Wang, H., Schmidt, R.A., Brandle, J.R., Litvina, I.V., and Jairell, R.L., 1997: "Pressure Perturbations around Shelterbelts: Measurements and Model Results", Preprints, 12th Symposium on Boundary Layers and Turbulence, American Meteorological Society, 563-564.

van Eimern, J., Karschon R., Razumova, L.A., and Robertson, G.W., 1964: Windbreaks and Shelterbelts. World Meteorol. Organ. Tech. Note No. 59. 188 pp.

Wang, H. and Takle, E.S., 1995: "Numerical Studies of Flow Through a Windbreak". Boundary Layer Meteorology 75, 141-173.

Wang, H., Takle, E.S., and Shen, J., 2001: "Shelterbelts and Windbreaks: Mathematical Modeling and Computer Simulation of Turbulent Flows", Annual Review of Fluid Mechanics 33, 549-586.

Wilson, J.D., 1985: "Numerical Studies of Flow Through a Windbreak", Journal of Wind Engineering and Industrial Aerodynamics 21, 119-154.

Wilson, J.D., 1987: "On the Choice of a Windbreak Porosity Profile", Boundary Layer Meteorology 38, 37-49.

Wilson J.D., 1997: "A Field Study of the Mean Pressure About a Windbreak", Boundary Layer Meteorology 85, 327-358.

Zhou, X.H., Brandle, J.R., Takle, E.S., and Mize, C.W., 2002: "Estimation of the Three-Dimensional Aerodynamic Structure of a Green Ash Shelterbelt", Agricultural and Forest Meteorology 111, 93-108.